Acta Pharmaceutica Sinica B 2024;14(12):5219–5234

Chinese Pharmaceutical Association
Institute of Materia Medica, Chinese Academy of Medical Sciences

Acta Pharmaceutica Sinica B

www.elsevier.com/locate/apsb
www.sciencedirect.com

ORIGINAL ARTICLE

# DNMT3A loss drives a HIF-1-dependent synthetic lethality to HDAC6 inhibition in non-small cell lung cancer

**Jiayu Zhang[a,†], Yingxi Zhao[a,†], Ruijuan Liang[a,†], Xue Zhou[b,†], Zhonghua Wang[a], Cheng Yang[a], Lingyue Gao[a], Yonghao Zheng[a], Hui Shao[a], Yang Su[c], Wei Cui[a], Lina Jia[a], Jingyu Yang[a], Chunfu Wu[a], Lihui Wang[a,*]**

[a]*Department of Pharmacology, School of Life Science and Biopharmaceutics, Shenyang Pharmaceutical University, Shenyang 110016, China*
[b]*Department of Biochemistry and Molecular Biology, School of Medical Devices, Shenyang Pharmaceutical University, Shenyang 110016, China*
[c]*Shengjing Hospital of China Medical University, Shenyang 110004, China*

Received 11 April 2024; received in revised form 18 June 2024; accepted 26 July 2024

**KEY WORDS**

*DNMT3A*;
NSCLC;
Synthetic lethal;
*HDAC6*;
HIF-1

**Abstract** *DNMT3A* encodes a DNA methyltransferase involved in development, cell differentiation, and gene transcription, which is mutated and aberrant-expressed in cancers. Here, we revealed that loss of *DNMT3A* promotes malignant phenotypes in lung cancer. Based on the epigenetic inhibitor library synthetic lethal screening, we found that small-molecule HDAC6 inhibitors selectively killed *DNMT3A*-defective NSCLC cells. Knockdown of *HDAC6* by siRNAs reduced cell growth and induced apoptosis in *DNMT3A*-defective NSCLC cells. However, sensitive cells became resistant when *DNMT3A* was rescued. Furthermore, the selectivity to HDAC6 inhibition was recapitulated in mice, where an HDAC6 inhibitor retarded tumor growth established from *DNMT3A*-defective but not *DNMT3A* parental NSCLC cells. Mechanistically, *DNMT3A* loss resulted in the upregulation of *HDAC6* through decreasing its promoter CpG methylation and enhancing transcription factor RUNX1 binding. Notably, our results indicated that HIF-1 pathway was activated in *DNMT3A*-defective cells whereas inactivated by HDAC6 inhibition. Knockout of *HIF-1* contributed to the elimination of synthetic lethality between *DNMT3A* and *HDAC6*. Interestingly, HIF-1 pathway inhibitors could mimic the selective efficacy of

*Corresponding author.
E-mail address: lhwang@syphu.edu.cn (Lihui Wang).
†These authors made equal contributions to this work.
Peer review under the responsibility of Chinese Pharmaceutical Association and Institute of Materia Medica, Chinese Academy of Medical Sciences.

https://doi.org/10.1016/j.apsb.2024.08.025

HDAC6 inhibition in *DNMT3A*-defective cells. These results demonstrated *HDAC6* as a HIF-1-dependent vulnerability of *DNMT3A*-defective cancers. Together, our findings identify *HDAC6* as a potential HIF-1-dependent therapeutic target for the treatment of *DNMT3A*-defective cancers like NSCLC.



## 1. Introduction

Cancer is considered as a genetic disease[1]. Gene mutations, including oncogenes and tumor suppressor genes (TSGs), play essential roles in the development and progression of cancer[2]. Driven mutation in oncogenes, such as *KRAS* and *EGFR*, would contribute to the malignant phenotype[3,4]. Similarly, the mutation in TSGs, such as *TP53* and *VHL*, usually results in the loss of their function, which would lead to the imbalance between oncogenes and TSGs, and further promote tumorigenesis[5,6]. In parallel with gene mutation, epigenetic alteration, through affecting gene expression, also plays a crucial role in cancer[7,8]. Interestingly, recent studies disclose that mutation in epigenetic enzymes is relatively frequent[9,10]. Thus, how to understand and take advantage of the frequent genetic mutation in epigenetic enzymes would be a crucial issue for the development of a novel anticancer approach.

DNA methyltransferase (DNMT), a kind of earlier discovered epigenetic enzyme, participates in DNA methylation to regulate various biological functions, including embryo development, cell differentiation, and gene transcription, and is associated with tumorigenesis[11-13]. Among DNMT family members, DNMT1, called maintenance DNMT, and DNMT3A and DNMT3B, called *de novo* DNMT, display the key role in the regulation of DNA methylation[14]. Although the inhibitors targeting DNMT, such as 5-azacytidine (5-AzaC) and 5-aza-2′-deoxycytidine (Decitabine)[15,16], have been applied in the treatment of leukemia[17,18], the impact of DNMTs on tumors and their therapeutic value are still controversial. A recent study discovered that the mutation rate of *DNMT3A* is the highest in the DNMT family, and mutation in *DNMT3A* was frequent in various tumors[19,20], which mostly resulted in loss of function (LOF) of *DNMT3A*[21]. However, the biological function and clinical value of *DNMT3A* LOF mutation in cancer need to be further explored.

With the introduction of the first DNA damage repair (DDR) based synthetic lethal drug (PARP inhibitor olaparib in cancer with *BRCA1* LOF mutation), research in DDR synthetic lethal has been an ideal strategy to target cancers with a mutation in certain DDR-related TSGs[22-24]. Previous studies revealed some potential DDR synthetic lethal gene pairs, such as *PTEN*/*CHD1*[25], *NOXA*/*RUNX1*[26], and *SLFN11*/*ATR*[27]. Similar to DDR gene pairs, epigenetic regulation enzymes also display interactive and complementary characteristics. Recently, some epigenetic synthetic lethal pairs were identified[28], including *ARID1A*/*ARID1B* and *ARID1A*/*EZH2*[29-31]. However, the epigenetic synthetic lethal gene pairs have not been studied extensively.

In this study, we revealed the TSG role of *DNMT3A* in lung cancer. In addition, histone deacetylase 6 (*HDAC6*), as a synthetic lethal partner of *DNMT3A* loss, was identified by utilizing an epigenetic inhibitor library. Interactively, *DNMT3A* loss would result in the upregulation of *HDAC6* by affecting its promoter cytosine-phosphate-guanine (CpG) methylation. Mechanistically, the hypoxia-inducible factor (HIF-1) pathway was found to be involved in this epigenetic synthetic lethal partner. These findings clarify the underlying mechanisms driving the malignant phenotype of *DNMT3A*-deficient lung cancer and broaden the field for the development of a novel epigenetic synthetic lethal strategy in cancer therapy.

## 2. Materials and methods

### 2.1. Cell culture

The human non-small cell lung cancer (NSCLC) cell lines A549, NCI-H460, NCI-H1299, and acute myeloid leukemia cell lines HL-60 and NB-4 were obtained from the American Type Culture Collection, and $DNMT3A^{KO}$ cells were constructed by our laboratory. Cell lines were cultured in RPMI 1640 Medium (Gibco, C11875500BT) supplemented with 10% fetal bovine serum (Gibco, 10270106) and 1% penicillin/streptomycin (Gibco,15140122).

### 2.2. Analysis of clinical specimens

Paraffin-embedded clinical tissue specimens from 80 lung adenocarcinoma patients were obtained from Shanghai Outdo Biotech. Clinical specimens used in this study were approved by the Committee for Ethical Review of Research Involving Human Subjects at Shanghai Biochip National Engineering Research Center (Ethical number: YB M-05-02). Written informed consent was obtained from the patients or their legal guardians before tissue sampling. The research design and methods were carried out in accordance with the Declaration of Helsinki's Guidelines and all applicable laws regarding the use of human study subjects. Among the 80 patients, 30 were determined as stage III, 47 were stage II, and 3 patients were stage I. The immunohistochemical staining of specimens was scored according to the intensity of dye color, the percentage of positive cells, and the calculated average score in studied cases. The scores above the average value were designated as high expression, and scores below the average were designated as low expression.

### 2.3. Epigenetics compound library screening

For screening, cells were seeded in 96-well plates at 2000−3000 cells/well and cultured overnight. The compounds (Med Chem Express, HY-L005) were added to the plates according to the concentration. After 72 h of drug treatment, viable cells were quantified with Cell-Counting-Kit-8 (Med Chem Express, HY-K0301) according to the manufacturer's instructions at indicated time points. All experiments were performed in triplicate.

### 2.4. Cell viability assay

For cell viability, cells were seeded in 96-well plates at 2000−3000 cells/well and cultured overnight. The agents were

added to the plates according to the concentration. After drug treatment, viable cells were quantified with Cell-Counting-Kit-8 (Med Chem Express, HY-K0301) according to the manufacturer's instructions at indicated time points. All experiments were performed in triplicate.

### 2.5. Colony formation assay

Cells were seeded in plates and incubated for 3 days, the agents were added to the plates with various concentrations. Every 2−3 days, fresh medium with agents was added to the plates. After culturing for 7−10 days, the cells were fixed with methanol for 15 min and stained with 0.1% crystal violet for half an hour, and the colonies were imaged and counted.

### 2.6. Apoptosis assay

For the assay of apoptotic cells, 0.2 million cells were seeded into 6-well plates and cultured overnight. After 72 h of drug treatment, cells were harvested and examined using an Annexin V−PI Apoptosis Detection Kit (BD, 556547) according to the manufacturer's protocol and analyzed by flow cytometry.

### 2.7. siRNA transfection

Cells were seeded into 6-well plates and cultured overnight. Cells were transfected with specific small interfering RNAs (siRNAs) according to the manufacturer's instruction (Thermo Fisher Scientific, L3000015) for 48−72 h. All siRNAs were obtained from BIONEER. The following siRNA sequences were used:
si*DNMT3A*#1: GCGUCACACAGAAGCAUAU
si*DNMT3A*#2: CCUCAGAGCUAUUACCCAA
si*HDAC6*#1: GAGGUAAAGAAGAAAGGCA
si*HDAC6*#2: CACUUCGAAGCGAAAUAUU
si*VHL*: UAUCACACUGCCAGUGUAUAC

### 2.8. Western blot analysis

Whole-cell lysates were isolated in RIPA buffer (Cell Signaling Technology, 9806S) supplemented with the protease inhibitor (Med Chem Express, HY-K0010) and the phosphatase inhibitor (Med Chem Express, HY-K0022). Total protein was separated on sodium dodecyl sulfate-polyacrylamide gel electrophoresis (SDS-PAGE) gels and then transferred onto polyvinylidene fluoride (PVDF) membranes. The membranes were blocked with 5% nonfat dried milk, and incubated with the indicated primary antibody and secondary antibodies. The protein bands were visualized with ECL detection reagents (PE, NEL105001EA). The primary antibodies used were anti-DNMT3A (Cell Signaling Technology, 32578), anti-HDAC6 (Cell Signaling Technology, 7558), anti-PARP (Santa Cruz, sc-7150), anti-HIF-1$\alpha$ (Proteintech, 20960-1-AP), anti-VHL (Proteintech, 24756-1-AP), anti-$\beta$-actin (anti-ACTB, Santa Cruz, sc-8432).

### 2.9. RNA isolation and quantitative real-time PCR (qRT-PCR)

Total RNA was isolated using TRIzol reagent (Invitrogen, 15596026) according to the manufacturer's protocol. First-strand cDNA synthesis was set up using the RevertAid First Strand cDNA Synthesis Kit (Thermo Fisher, K1622). Quantitative real-time PCR analysis was performed by using Top Green qPCR SuperMix (Transgene, AQ601-04) by the manufacturer's protocols. *GAPDH* was used as the endogenous control. All qRT-PCRs were set up in triplicates using three biological replicates for each sample.

### 2.10. Immunohistochemical staining

Tumor samples acquired from the mice bearing H460/H1299 cells were fixed in 4% neutral buffered formalin and embedded in paraffin. Samples were dewaxed, and hydrated with xylene and ethanol, and citric acid buffer was used for antigen repair. Tumor samples were incubated with primary antibody and secondary antibody. DAB and hematoxylin were added for staining and observed under a microscope. The primary antibodies used were anti-DNMT3A (Proteintech, 20954-1-AP), anti-HDAC6 (Proteintech, 12834-1-AP), anti-Ki67 (Abcam, ab15580), anti-HIF-1$\alpha$ (Proteintech, 20960-1-AP), anti-VHL (Proteintech, 24756-1-AP).

### 2.11. In vivo tumor xenograft animal model

BALB/c nude mice (body weight 18−22 g) were maintained in a specific-pathogen-free (SPF) facility. NCI-H460/H1299 cells ($1 \times 10^6$−$2 \times 10^6$ cells in 0.2 mL phosphate-buffered saline) were subcutaneously injected into the right flank of BALB/c nude mice. The drugs were administered to mice by intraperitoneal injection for 21 consecutive days. After 21 days, the mice were sacrificed, the tumors were photographed and the tumor volumes were analyzed. Tumor volumes were measured using calipers every 2 days and calculated by Eq. (1):

$$\text{Tumor volume} = 1/2 \times (\text{Long diameter}) \times (\text{Short diameter})^2 \quad (1)$$

### 2.12. Statistical analysis

Statistical analyses were performed using SPSS V 26.0 software. Data in all graphs were represented as mean ± standard error of mean (SEM) of biological triplicates by using GraphPad Prism version 8.0. Statistical significance was determined by Student's *t*-test (independent samples *t*-test), one-way analysis of variance (ANOVA) followed by Tukey's or Dunnett's T3 multiple comparisons test. $P$ values $< 0.05$ were considered statistically significant.

## 3. Results

### 3.1. The aberrant alteration and the role of DNMT3A in cancer

Due to the paradoxical role of *DNMT3A* in cancer, we analyzed the expression and clinical significance of *DNMT3A* in various cancers according to the Kaplan−Meier Plotter database. As shown in Fig. 1A, the median survival of patients with low expression of *DNMT3A* was 56 months compared to 99 months for patients with high *DNMT3A* expression. The patients with the decreased expression of *DNMT3A* predict a poor prognosis, suggesting the TSG role of *DNMT3A* in cancer. The inactivation of TSGs is mostly caused by mutation. Therefore, we assessed the clinical value of *DNMT3A* mutation using the ICGC database. Our analyzed data indicated that there was a 12.0% frequency of *DNMT3A* mutation in cancer. Importantly, mutation of *DNMT3A* was associated with poor prognosis (Fig. 1B), which further confirmed its possible TSG role in cancer. According to the

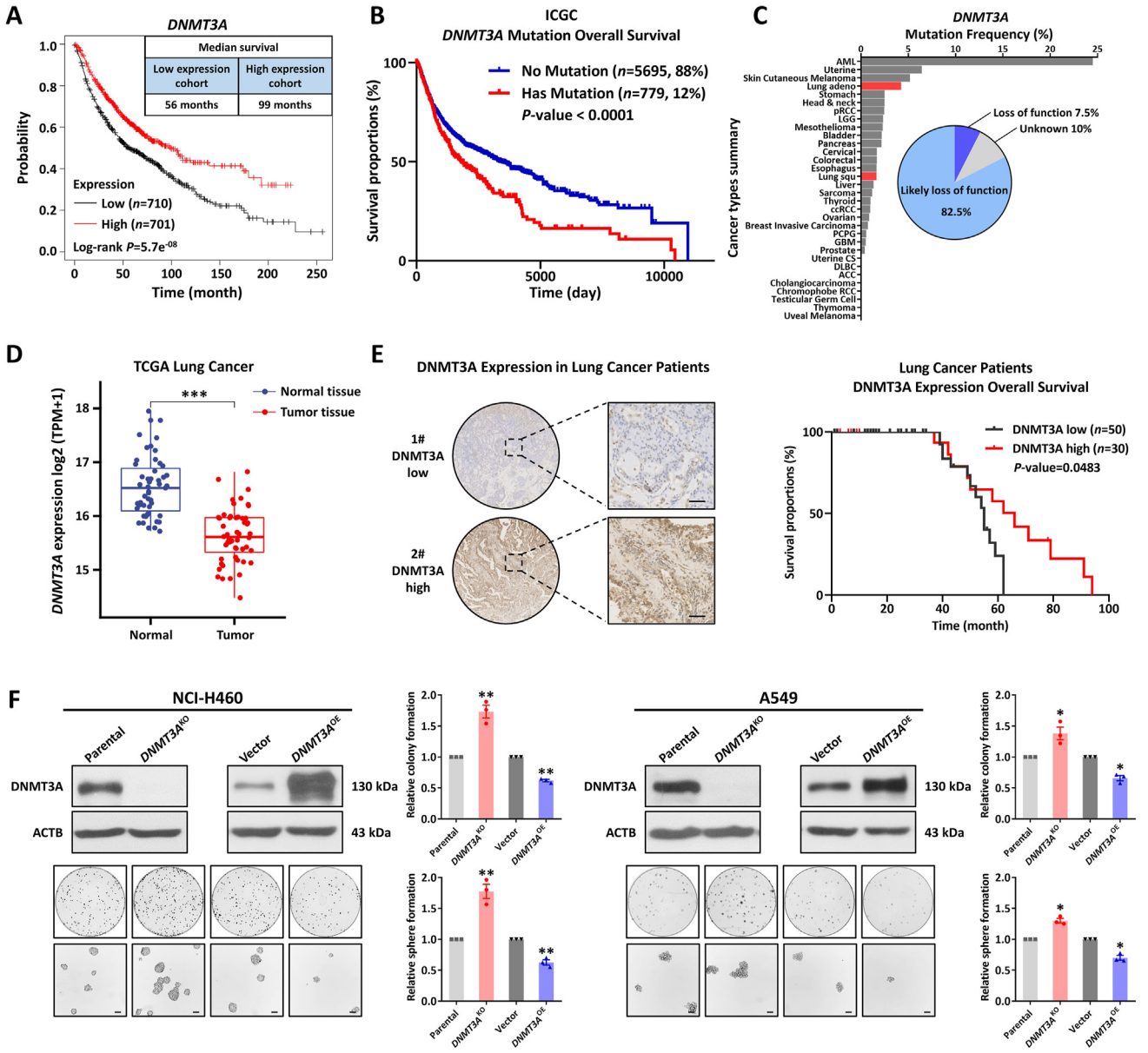


**Figure 1** Effects of *DNMT3A* deletion on the biological characteristics of non-small cell lung cancer. (A) The correlation between *DNMT3A* expression and survival probability is shown. Log-rank (Mantel−Cox) test, $P < 0.001$. (B) The overall survival of lung cancer patients with *DNMT3A* mutation ($n = 779$) and no *DNMT3A* mutation ($n = 5695$). Log-rank (Mantel−Cox) test, $P < 0.001$. (C) The incidence of *DNMT3A* mutations in 32 types of cancer (10,967 samples, lung adenocarcinoma 4.24% and lung squamous cell carcinoma 1.64%). The majority of *DNMT3A* mutations are loss of function or likely loss of function. (D) The expression of *DNMT3A* in normal tissues ($n = 50$) and tumor tissues ($n = 51$) in the TCGA database. Log-rank (Mantel−Cox) test, $^{***}P < 0.001$. (E) The correlation between DNMT3A protein expression level and overall survival in lung cancer is shown. The sections of tumor tissues from two lung cancer patients showed the immunohistochemical detection of DNMT3A protein. Scale bars, 50 μm. Log-rank (Mantel−Cox) test, $^{*}P < 0.05$. (F) Expression of DNMT3A in *DNMT3A* knockout and overexpression cells, and effect of DNMT3A expression on cell proliferation and self-renewal ability. Data are presented as mean ± SEM ($n = 3$). $^{*}P < 0.05$, $^{**}P < 0.01$. *P* values were determined using Student's *t*-test (independent samples *t*-test).

mutation rate of *DNMT3A* in various tumors, lung cancer is located in the front ranks (Fig. 1C and Supporting Information Fig. S1). Thus, we next choose lung cancer as a study example. TCGA database revealed that, compared with normal tissues, lung cancer tissues expressed *DNMT3A* at a lower level (Fig. 1D). Furthermore, we measured the expression level of DNMT3A in 80 patients of lung cancer. In line with the database data, patients with DNMT3A low expression predicted a bad survival rate in lung cancer (Fig. 1E). To explore the function of *DNMT3A* in lung cancer, we established the *DNMT3A* knockout (*DNMT3A*$^{KO}$) model using the CRISPR-Cas9 approach. As expected, knockout of *DNMT3A* resulted in an enhanced ability in proliferation and self-renewal in H460 and A549 cell lines (Fig. 1F). On the contrary, overexpression of *DNMT3A* would lead to the reduction of proliferation and self-renewal in H460 and A549 cell lines (Fig. 1F). Taken together, the above results indicate that the

aberrant alteration of *DNMT3A* is frequent and *DNMT3A* may act as a tumor suppressor gene in lung cancer, which suggests the crucial role of *DNMT3A* in cancer.

### 3.2. *Knockout of DNMT3A induces tumor growth and drug resistance*

To further explore the role of *DNMT3A* in lung cancer, we established subcutaneous xenograft models with NCI-H460 parental and *DNMT3A*$^{KO}$ cells. As expected, knockout of *DNMT3A* resulted in rapid tumor growth in a mouse model. Compared with the parental H460 xenograft model, the H460-*DNMT3A*$^{KO}$ xenograft displayed an increasing tumorigenesis capability (Fig. 2A). In addition, the proliferation biomarker, Ki67, was increased in H460-*DNMT3A*$^{KO}$ tumor tissues as compared with parental H460 tumor tissues (Fig. 2B), which confirmed the TSGs role of *DNMT3A* in lung cancer. Previous studies indicated that epigenetic enzyme mutation would contribute to drug resistance[32], therefore, we next assessed the effects of gene manipulation of *DNMT3A* on drug sensitivities in lung cancer. As shown in Fig. 2C, knockout of *DNMT3A* resulted in the decrease of sensitivities of H460 and A549 cell lines to frequently-used chemotherapy agents, including cisplatin (CDDP), etoposide (VP-16), paclitaxel (PTX) and vincristine (VCR), whereas overexpression of *DNMT3A* could increase the sensitivities of H460 and A549 cell lines to chemotherapy agents. Consistent with the *in vitro* results, the H460-*DNMT3A*$^{KO}$ xenograft mouse model also showed a reduction of sensitivities to chemotherapy agents, including cisplatin, paclitaxel, and DNMT inhibitor decitabine, as compared with the parental xenograft model (Fig. 2D and Supporting Information Fig. S2A). Moreover, the weight of mice did not decrease significantly (Fig. S2B). The above results demonstrate that *DNMT3A* exhibits a TSG role in lung cancer.

### 3.3. *Identification of a synthetic lethal interaction of DNMT3A and HDAC6*

Based on the above finding, we next performed a drug screening with a total of 443 epigenetic enzyme inhibitors in *DNMT3A*

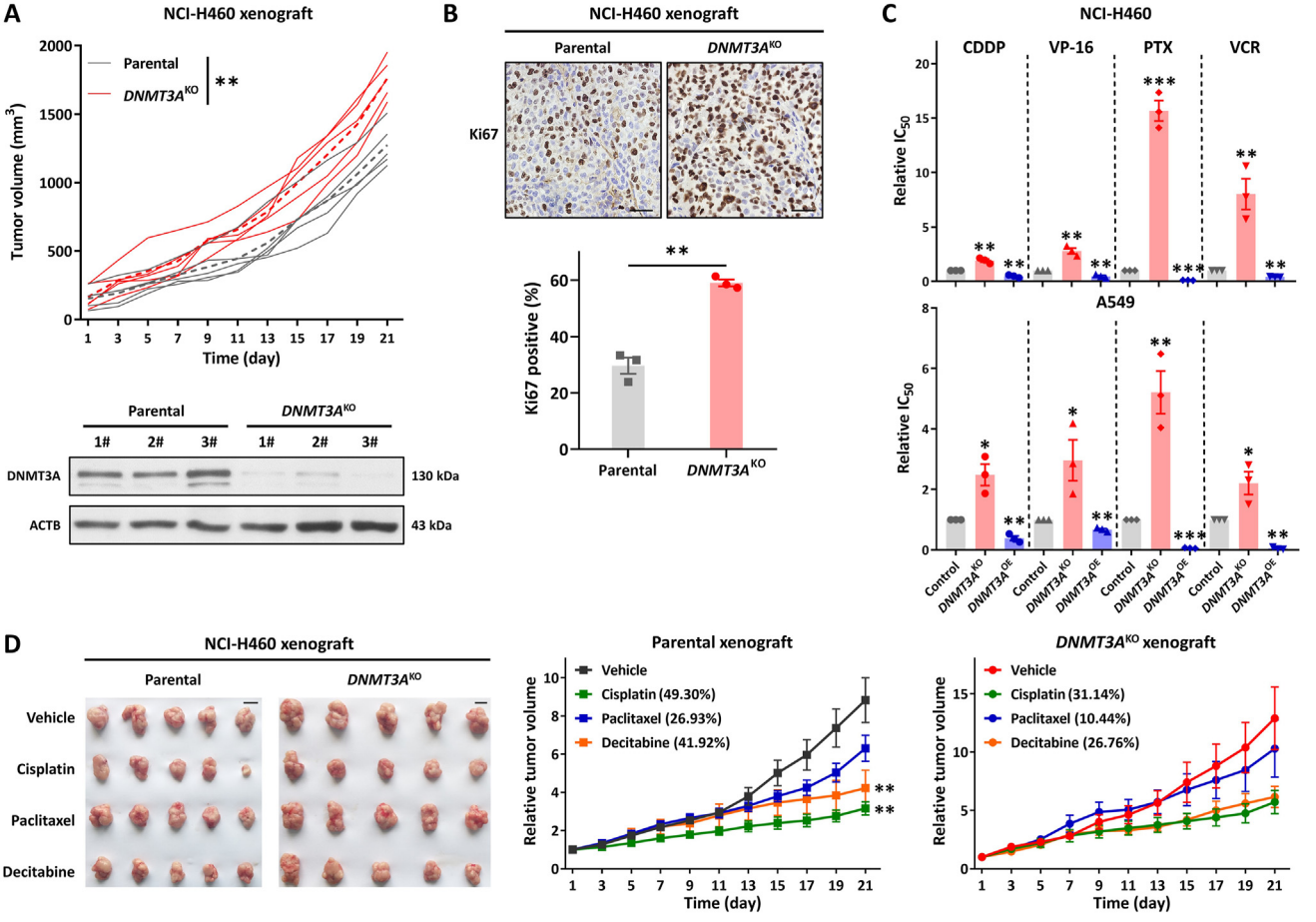


**Figure 2** Knockout of *DNMT3A* promotes tumor growth and drug resistance *in vivo*. (A) Tumor growth in BALB/c-nu mice xenografted with NCI-H460-*DNMT3A*$^{KO}$ and parental cells ($n = 5$). The expression level of DNMT3A in mouse tumor tissues (B) Ki67 staining of tumor tissue cells in xenograft mice. Scale bars, 25 μm. (C) Effect of DNMT3A expression on the sensitivity of chemotherapeutic drugs (CDDP, VP-16, PTX, and VCR). (D) CDX-bearing mice ($n = 5$ mice per group) were treated with vehicle (three times per week), CDDP (4 mg/kg, twice per week), PTX (5 mg/kg, twice per week), or decitabine (1 mg/kg, three times per week) through intraperitoneal administration. The graph shows the tumor image and relative tumor volume, with the tumor growth inhibition value. Scale bars, 1 cm. Data are presented as means ± SEM ($n = 3$–5). $^*P < 0.05$, $^{**}P < 0.01$, $^{***}P < 0.001$. In (A) and (B), $P$ values were determined using Student's $t$-test (independent samples $t$-test). In (C) and (D), $P$ values were determined using one-way ANOVA with Tukey's or Dunnett's T3 multiple comparisons test.

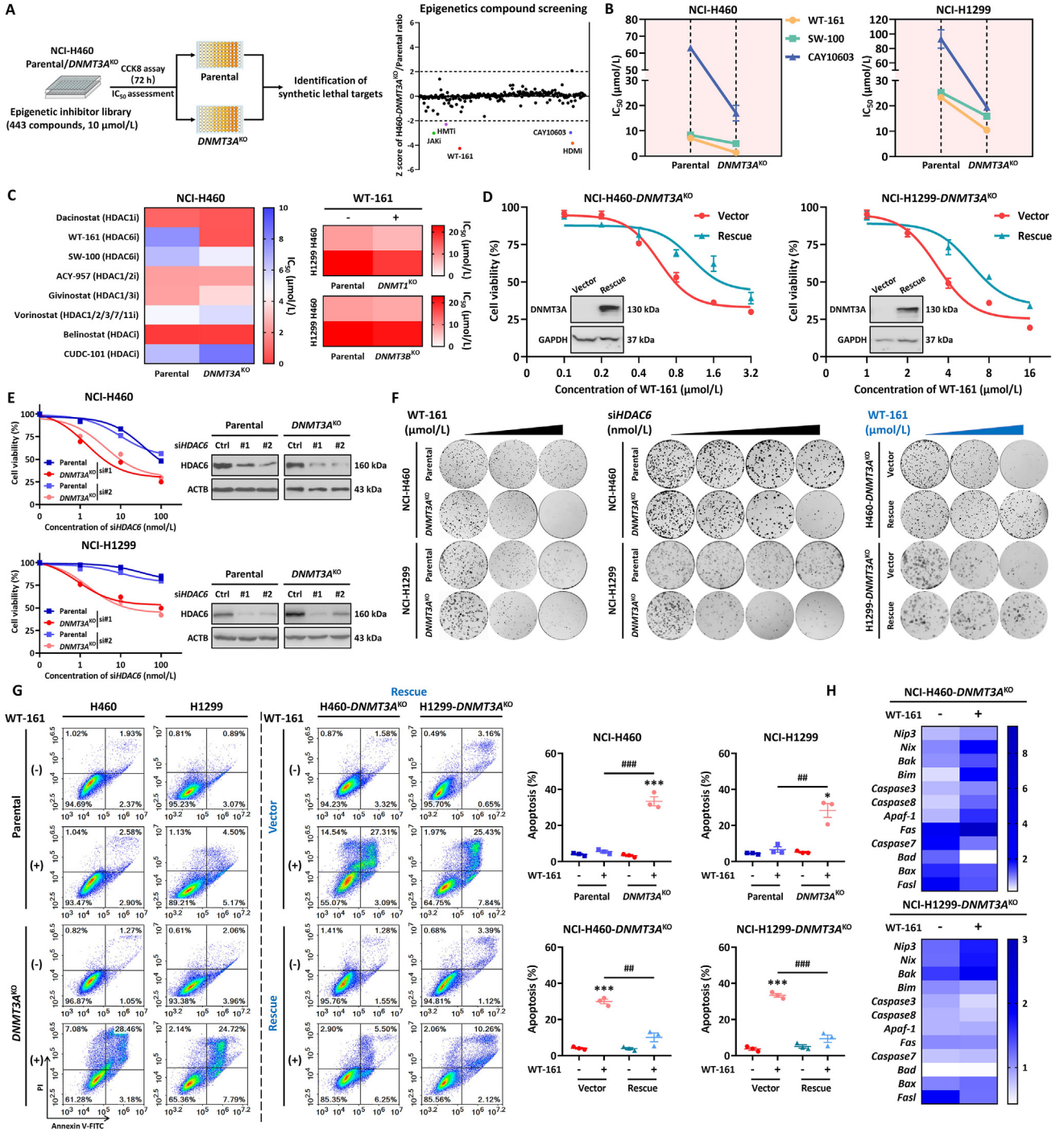


**Figure 3** Identification and validation of synthetic lethal target. (A) Flow chart for synthetic lethality screening of epigenetics compound library. After NCI-H460 parental and *DNMT3A*$^{KO}$ cell lines were treated with epigenetics compound library (10 μmol/L) for 72 h, cell viability was determined by CCK8 assay. *Z*-score scatterplot of relative lethality for epigenetics compound library screening. Most compounds have a *Z*-score index between 1 and −1, and compounds with a *Z*-score below −2 were deemed "hit". In (A), 256 compounds are shown (the remaining 187 compounds are shown in Supporting Information). (B) NCI-H460/NCI-H1299 parental and *DNMT3A*$^{KO}$ cells were treated with HDAC6 selective inhibitors (WT-161, SW-100, CAY10603) for 72 h, and the cell viability was detected by CCK8 assay. (C) A heatmap showing the $IC_{50}$ values of the selected compound on NCI-H460 parental and *DNMT3A*$^{KO}$ cells (left), and the efficacy of WT-161 in NCI-H460/NCI-H1299 parental or *DNMT1*$^{KO}$/*DNMT3B*$^{KO}$ cells (right). (D) Effect of DNMT3A re-expression on the synthetic lethality of the HDAC6 inhibitor in NCI-H460-*DNMT3A*$^{KO}$ and NCI-H1299-*DNMT3A*$^{KO}$ cells. (E) The cell viability of parental and *DNMT3A*$^{KO}$ cells after gene intervention of HDAC6 expression. (F) Effects of HDAC6 inhibition (0, 0.16, 0.32 μmol/L for H460 and 0, 2, 4 μmol/L for H1299) or knockdown (0, 20, 40, 60 nmol/L for H460 and H1299) on the colony formation ability of lung cancer cells with different DNMT3A expression levels. (G) The apoptosis induction by HDAC6 inhibitor WT-161 (0, 1 μmol/L for H460 and 0, 5 μmol/L for H1299) in lung cancer cells with different DNMT3A expression levels.

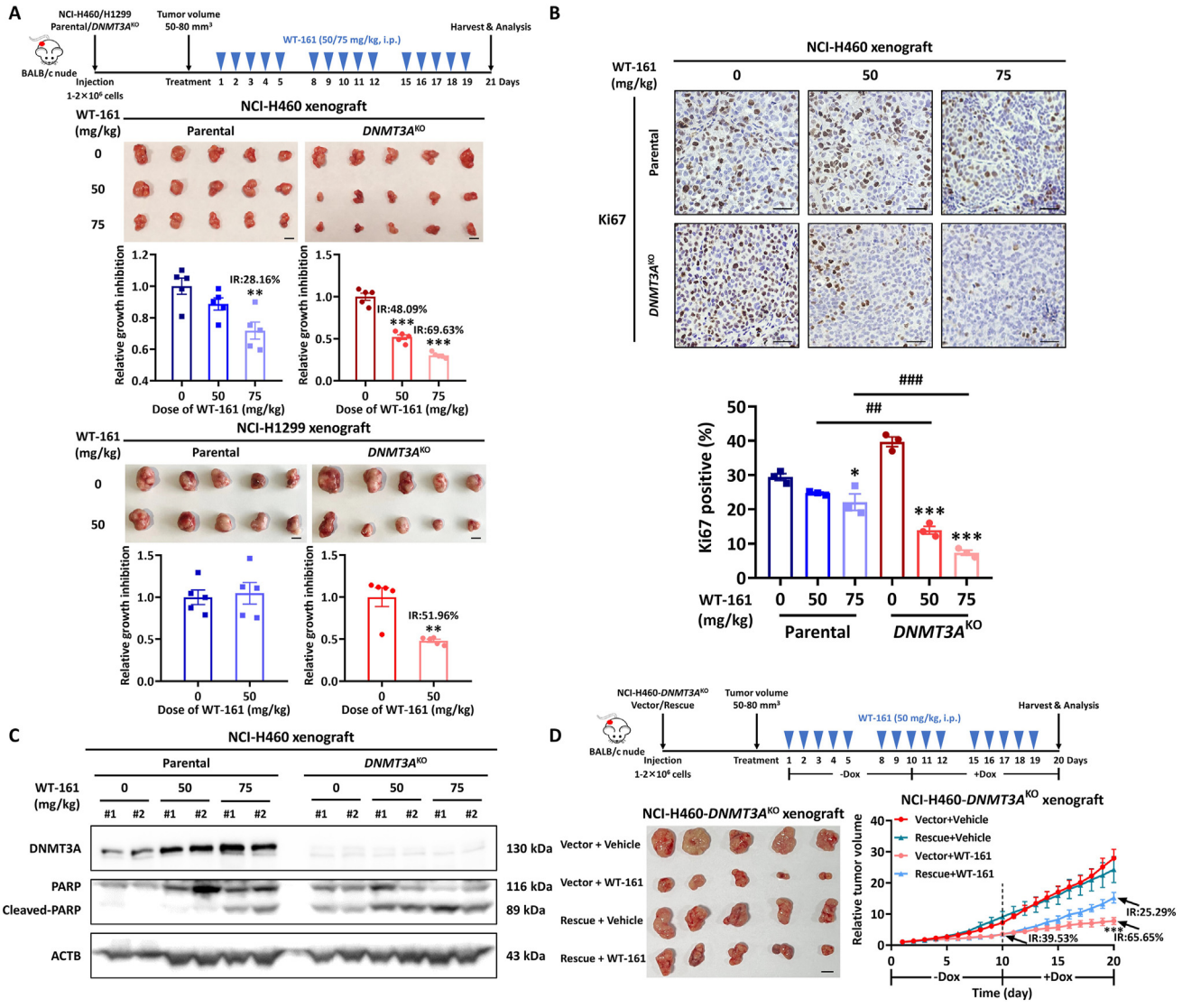


**Figure 4** HDAC6 inhibition by WT-161 is effective in *DNMT3A*-deficient NSCLC mouse model. (A) Representative images of NCI-H460/NCI-H1299 parental and *DNMT3A*$^{KO}$ xenograft tumors and statistical analysis of the relative growth inhibition ($n = 5$). Scale bars, 1 cm. (B) Evaluation of Ki67 expression in the indicated xenograft tumors by IHC assay. Scale bars, 25 μm. The statistics of Ki67 positive cell rate in the indicated xenograft tumors are shown at the bottom. (C) Western blot analysis of DNMT3A and PARP expression in NCI-H460 parental and *DNMT3A*$^{KO}$ xenograft tumors. (D) Image of a tumor xenograft model with DNMT3A expression induced by doxycycline, 1−10 days without doxycycline induction and 11−20 days with doxycycline induction. The tumor growth curve is shown on the right ($n = 5$). Data are presented as means ± SEM ($n = 3$−5). $^{*}P < 0.05$, $^{**}P < 0.01$, $^{***}P < 0.001$, compared with control group. $^{\#\#}P < 0.01$, $^{\#\#\#}P < 0.001$, compared with the indicated group. *P* values were determined using Student's *t*-test (independent samples *t*-test) and one-way ANOVA with Tukey's or Dunnett's T3 multiple comparisons test.

proficient (parental) and *DNMT3A*$^{KO}$ cells to identify an epigenetic synthetic lethal partner with TSG *DNMT3A*. Drug testing and viability assay were conducted with a single concentration of 10 μmol/L. To exclude the effect of high selectivity but with low efficacy, we used the *Z* score to assess the selectivity of compounds. Out of 443 compounds, we identified 5 inhibitors that showed higher efficiency in H460-*DNMT3A*$^{KO}$ cells compared with parental cells. Notably, within the identified hits, we found JAKi, which is in line with previous reports (Fig. 3A and Supporting Information Fig. S3A)[33]. Among the 5 identified inhibitors, two inhibitors, namely WT-161 and CAY10603, belong to HDAC6-specific inhibitors. The selective action of HDAC6 inhibition was confirmed by various inhibitors targeting HDAC6 in both H460-*DNMT3A*$^{KO}$ and H1299-*DNMT3A*$^{KO}$ cell lines (Fig. 3B). To clarify the specific action of HDAC6 inhibition, we also detected the cell viability of parental and *DNMT3A*$^{KO}$ cell

(H) The heatmap showed the changes of apoptosis-related target genes in NCI-H460-*DNMT3A*$^{KO}$ and NCI-H1299-*DNMT3A*$^{KO}$ under WT-161 treatment. Data are presented as means ± SEM ($n = 3$). $^{*}P < 0.05$, $^{***}P < 0.001$, compared with control group. $^{\#\#}P < 0.01$, $^{\#\#\#}P < 0.001$, compared with the indicated group. *P* values were determined using Student's *t*-test (independent samples *t*-test).

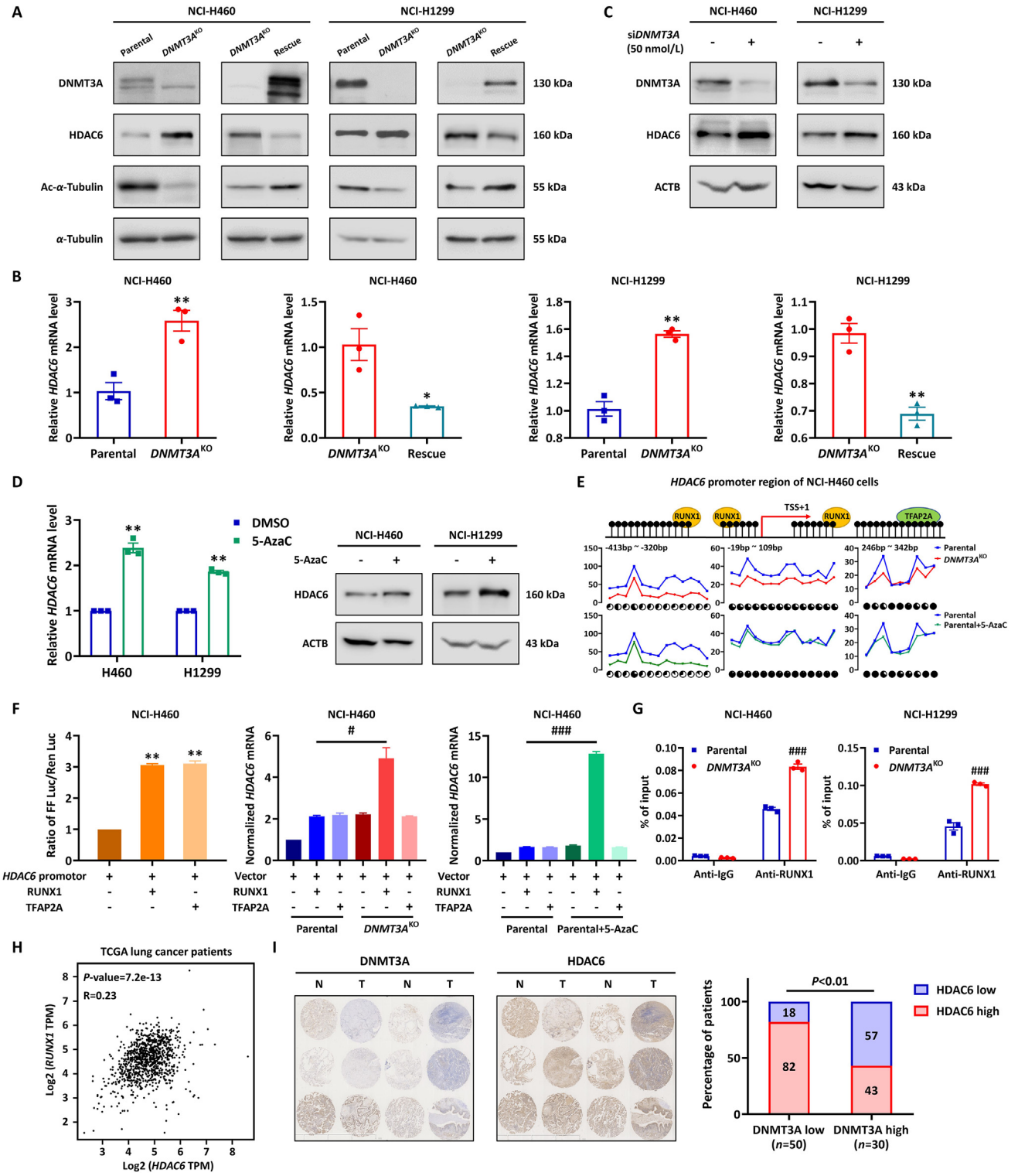


**Figure 5** DNMT3A inhibition induces HDAC6 through reducing promoter methylation status. (A) Expression level and activity of HDAC6 in NCI-H460/H1299 with different DNMT3A expression levels. (B) Relative *HDAC6* mRNA level in NCI-H460/H1299 with different DNMT3A expression levels. (C) HDAC6 protein expression level in NCI-H460/H1299 cells after knockdown of *DNMT3A* by siRNA (50 nmol/L). (D) Changes of *HDAC6* mRNA and protein levels in NCI-H460/NCI-H1299 parental cells treated with 5-azacytidine (10 μmol/L for H460 and 5 μmol/L for H1299, 24 h). (E) Predicted transcription factor binding site and bisulfite sequencing analysis in *HDAC6* promoter region. Bisulfite sequencing was used to analyze the altered methylation status in the CG site of *HDAC6* promoter under different DNMT3A expression levels. 5-Azacytidine treated with 5 μmol/L for 24 h. (F) Dual luciferase reporter assay and RT-qPCR were used to evaluate *HDAC6* promoter activity and mRNA levels after overexpression of transcription factors in different DNMT3A expression states. (G) The binding of RUNX1 to *HDAC6* promoter in parental and *DNMT3A*$^{KO}$ cells was detected by ChIP-qPCR. (H) The correlation between *RUNX1* and *HDAC6* expression was

lines after being treated with additional HDAC inhibitors. The results indicated that only HDAC6-specific inhibitors displayed a selectivity inhibitory action to *DNMT3A*$^{KO}$ cell lines (Fig. 3C). Furthermore, we also evaluated the HDAC6 inhibition in other DNMT isoforms (*DNMT1* and *DNMT3B*) knockout cells. As shown in Fig. 3C and Fig. S3B, treatment with HDAC6 inhibitor WT-161 exhibited a similar inhibitory action in both parental and *DNMT1*$^{KO}$ or *DNMT3B*$^{KO}$ cell lines. The above results indicate synthetic lethal action between *DNMT3A* and *HDAC6* is a specific and unique interaction. To confirm that the selective action of HDAC6 inhibition on NSCLC cell growth was due to the on-target effect of *DNMT3A* deficiency, we restored *DNMT3A* expression in *DNMT3A*$^{KO}$ cell lines and found that DNMT3A expression reduced the sensitivity of cells to WT-161 (Fig. 3D), demonstrating the on-target effect of the *DNMT3A* construct. Together these data elucidated that HDAC6 inhibition selectively reduces the growth of *DNMT3A*-deficient NSCLC cells.

### 3.4. *HDAC6 inhibition reduces the growth of DNMT3A-deficient NSCLC cells by inducing cell apoptosis*

Given that pharmacology inhibition of HDAC6 by compounds might be mediated by off-target action, we next assayed whether specific siRNA for *HDAC6* produced a selective action in *DNMT3A*-deficient NSCLC cells. As shown in Fig. 3E, knockdown of *HDAC6* by two siRNAs could result in an obvious concentration-dependent reduction of cell growth in both *DNMT3A*$^{KO}$ cell lines, but just produced a weak decrease in parental cell lines, which mimicked the action of HDAC6 inhibitors. To further assess the synthetic lethal action between *DNMT3A* and *HDAC6*, we also performed colony formation analysis. Our results revealed that consistent with cell viability data, inhibition of HDAC6 by both pharmacology inhibitor and gene manipulation led to selective reduction of colony formation number in H460-*DNMT3A*$^{KO}$ and H1299-*DNMT3A*$^{KO}$ cell lines, whereas restoration of *DNMT3A* in *DNMT3A*$^{KO}$ cell lines alleviate their inhibitory action (Fig. 3F). Next, to explore the underlying mechanism, we detected the cell apoptosis status, which is considered as the main death pathway of synthetic lethal, after being treated with pharmacology inhibitors or given gene manipulation. The apoptosis measurement data indicated that HDAC6 inhibitor WT-161 treatment resulted in an obvious increase of apoptosis rate (Annexin V positive cell), from ~2% to ~31%, in H460-*DNMT3A*$^{KO}$ cells, compared that, from ~4% to ~5%, in H460 parental cells. Similar results were obtained from H1299 parental and *DNMT3A*$^{KO}$ cell lines (Fig. 3G). Consistent with pharmacology inhibitor treatment, the addition of specific *HDAC6* siRNA also led to selectively increasing cell apoptosis in *DNMT3A*$^{KO}$ cells (Fig. S3C). The *DNMT3A*-deficient-dependent apoptosis induction of HDAC6 inhibition was further confirmed by the restoration of *DNMT3A* (Fig. 3G). Rescue of *DNMT3A* significantly alleviated the apoptosis rate, from ~30% to ~10%, in H460/H1299-*DNMT3A*$^{KO}$ cell lines. To further validate the synthetic lethal effect of *DNMT3A* and *HDAC6*, we found that the hotspot mutation *DNMT3A* R882H in acute myeloid leukemia (AML) is a loss-of-function mutation[34]. We introduced *DNMT3A* R882H into lung cancer cell lines H460 and H1299 to simulate the real *DNMT3A* LOF mutation in the clinic as much as possible and then investigated the effect of the HDAC6 inhibitor WT-161 on cells expressing the R882H mutation. The results showed that similar to the effect of WT-161 on *DNMT3A* knockout cells, WT-161 selectively inhibited the growth of cells expressing R882H. This indicated that HDAC6 inhibitor selectively killed cells with DNMT3A functional defects (Supporting Information Fig. S4A and S4B). Moreover, we selected two AML cell lines HL-60 and NB-4, treated cells with siRNAs to silence *DNMT3A*, and assessed the effect of WT-161 on AML cells. The results also confirmed the synthetic lethality of *DNMT3A*/*HDAC6* in AML cells (Fig. S4C and S4D). In addition, we also found that some apoptosis-related genes were up-regulated in *DNMT3A*$^{KO}$ cells treated with WT-161 (Fig. 3H). Taken together, the above results demonstrated that inhibition of HDAC6 by both pharmacology inhibitor and gene manipulation could selectively reduce cell viability in *DNMT3A*$^{KO}$ cells by inducing cell apoptosis.

### 3.5. *HDAC6 inhibition by WT-161 is effective in DNMT3A-deficient NSCLC mouse model*

To validate whether HDAC6 inhibition could be effective *in vivo*, we evaluated the efficacy of HDAC6 inhibitor WT-161 in mice carrying H460 and H1299 NSCLC xenografts (Fig. 4A). WT-161 treatment resulted in a significant reduction in tumor volume in the *DNMT3A*$^{KO}$ xenograft model, whereas the parental xenograft model did not change in tumor volume. Similarly, WT-161 administration also led to a dose-dependent decrease in tumor volume (Fig. 4A), with a maximal inhibition rate (IR) of 69.63%, and positive expression of Ki67 (Fig. 4B). Importantly, the administration of WT-161 also significantly induced apoptosis measured by cleaved PARP in H460-*DNMT3A*$^{KO}$ xenograft tumors compared to that in parental xenograft tumors (Fig. 4C). To further explore the role of the DNMT3A in the anti-tumor efficacy of HDAC6 inhibition *in vivo*, we applied the Tet-on model to animal experiments. The results showed that in the absence of doxycycline (dox) induction, after treatment with WT-161, the tumor growth in H460-*DNMT3A*$^{KO}$ xenograft mice was significantly decreased, with IR 39.53% (Fig. 4D). After the addition of the inducer to rescue *DNMT3A* expression, the tumor inhibitory efficacy of WT-161 in mice receiving H460-*DNMT3A*$^{KO}$ cells was significantly weaker than that in the vector-construct group (IR: 25.29% *vs.* 65.65%), supporting *DNMT3A* deficiency as an essential contributor of WT-161 efficacy (Fig. 4D). The body weight and viscera index of the H460-*DNMT3A*$^{KO}$ xenograft model were not significantly altered during drug administration (Supporting Information Fig. S5). Taken together, these data indicate that HDAC6 inhibition by WT-161 is effective in

analyzed by the GEPIA database (lung adenocarcinoma and lung squamous cell carcinoma). (I) Immunohistochemistry combined with Pearson correlation analysis was used to analyze the correlation between the expression of DNMT3A and HDAC6 in the tumor tissues of 80 patients. N: Normal tissue, T: Tumor tissue. Data are presented as means ± SEM ($n = 3$). *$P < 0.05$, **$P < 0.01$, compared with control group. $^{\#}P < 0.05$, $^{\#\#\#}P < 0.001$, compared with the indicated group. $P$ values were determined using Student's $t$-test (independent samples $t$-test) and one-way ANOVA with Tukey's or Dunnett's T3 multiple comparisons test.

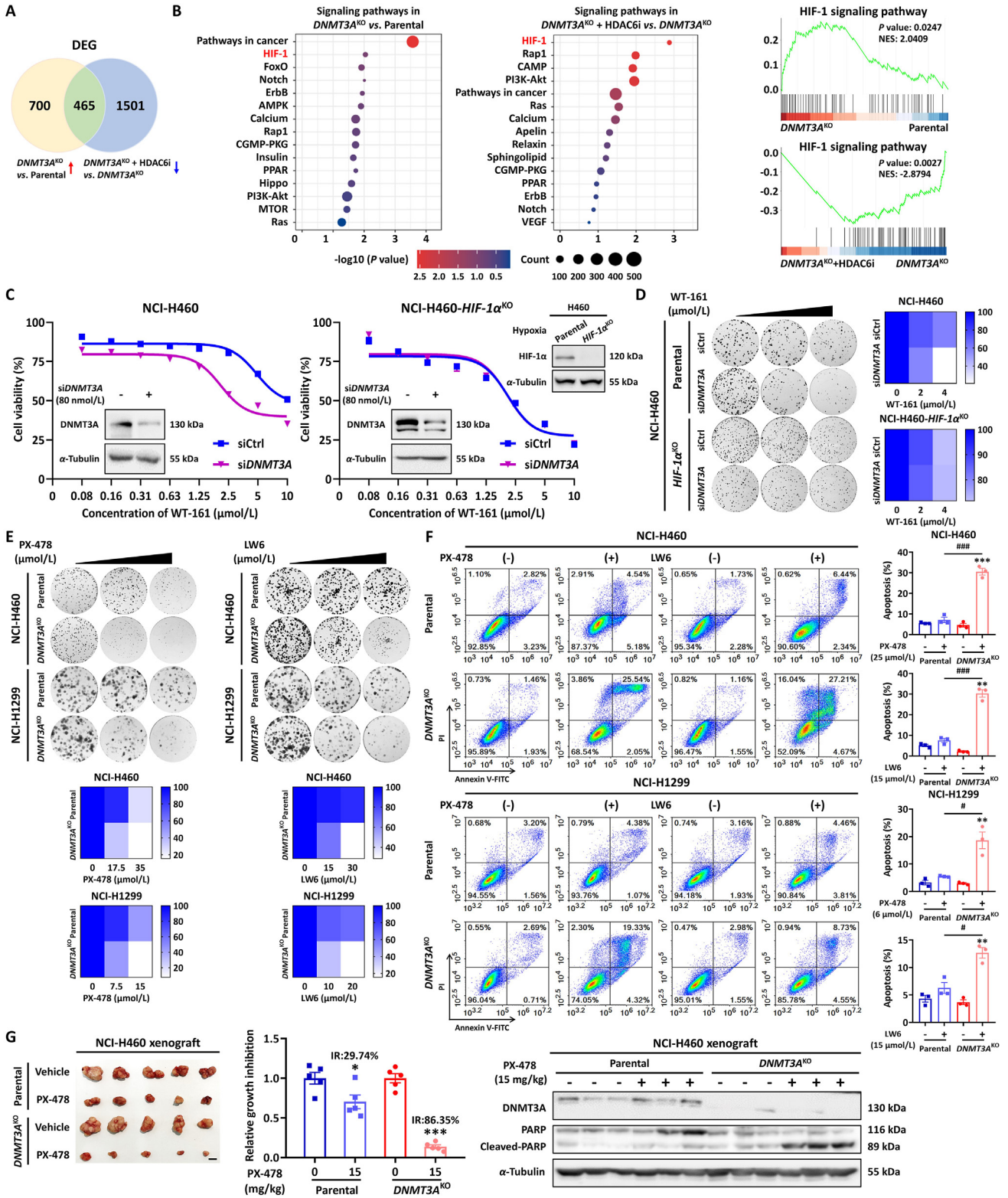


**Figure 6** *DNMT3A* deficiency results in HDAC6−VHL−HIF-1 axis activation. (A) The Venn diagram shows the differentially expressed genes (DEG) between *DNMT3A*$^{KO}$ *vs.* parental and *DNMT3A*$^{KO}$ + WT-161 (2.5 μmol/L, 48 h) *vs. DNMT3A*$^{KO}$. (B) The bubble map and GSEA analysis showed the most obvious signaling pathway with different conditions. (C) *DNMT3A* was knocked down by siRNA (80 nmol/L) in NCI-H460 parental and *HIF-1α*$^{KO}$ cells and cell activity was detected by CCK8 after treatment with WT-161 for 48 h. (D) A colony formation assay was used to investigate the changes in the proliferation ability of NCI-H460 parental and *HIF-1α*$^{KO}$ cells after *DNMT3A* knockdown. (E) HIF-1α inhibitors (PX-478 and LW6) were treated on NCI-H460/NCI-H1299 parental and *DNMT3A*$^{KO}$ cells, and the proliferation ability of the cells was investigated by colony formation assay. (F) Annexin V-PI staining showed changes in apoptotic ability of NCI-H460/NCI-H1299 parental and

*DNMT3A*-deficient NSCLC mouse models by suppressing cell proliferation and inducing cell apoptosis.

### 3.6. *DNMT3A inhibition induces HDAC6 through reducing promoter methylation status*

Understanding the mode of interaction of synthetic lethal partners is critical for the formulation of clinical therapeutic strategy. To address this issue, we next explored how knockout of *DNMT3A* affects HDAC6 expression. As shown in Fig. 5A, the protein expression and activity of HDAC6 were obviously upregulated in *DNMT3A*-deficient NSCLC cell lines as compared with parental cell lines. On the contrary, the other HDACs' isoforms were not significantly changed (Supporting Information Fig. S6). Additionally, the restoration of *DNMT3A* would lead to the down-regulation of HDAC6 protein in *DNMT3A*-deficient NSCLC cell lines (Fig. 5A). This expression pattern was mimicked at the mRNA level (Fig. 5B), supporting *HDAC6* induction by DNMT3A inhibition at transcription regulation. Notably, knockdown of *DNMT3A* by siRNA also resulted in the upregulation of HDAC6 (Fig. 5C), which further confirmed the regulation relationship between DNMT3A and HDAC6. In view of the role of DNMT3A in DNA methylation, we next detected the expression of *HDAC6* after being treated with DNMT inhibitor 5-AzaC in NSCLC cell lines. As shown in Fig. 5D, treatment with 5-AzaC would induce the upregulation of *HDAC6* in both mRNA and protein levels, demonstrating that the expression of HDAC6 might be regulated by DNA methylation. Usually, DNA methylation in the promoter region could block transcription factor's binding and contribute to transcription suppression[35]. Therefore, we next analyzed the transcription factor binding site in the *HDAC6* promoter region using the JASPAR prediction system. The analyzed results indicated that transcription factors RUNX1 and TFAP2A own a relatively higher matrix score (Fig. 5E). Next, we investigated whether the transcription factors could regulate the transcription activation of *HDAC6*. Our results indicated that the reporter gene of *HDAC6* promoter could be activated by overexpression of RUNX1 and TFAP2A in H460 cells, and their activation can be enhanced by treatment with 5-AzaC (Fig. 5F), suggesting the status of promoter methylation of *HDAC6* might affect its transcription activation by transcription factors. In addition, the transcription level of *HDAC6* was also enhanced by RUNX1 overexpression, but not TFAP2A, in the *DNMT3A*$^{KO}$ cells and 5-AzaC treated cells (Fig. 5F), which indicated that RUNX1 played a more important role in methylation-dependent HDAC6 regulation. To deeply explore the interaction between DNA methylation and transcription factor in the *HDAC6* promoter region, we performed bisulfite sequencing analysis. Our data revealed that, as compared with parental cells, there were 3 sequencing regions, containing transcription factor binding sites, in the *HDAC6* promoter that showed a decrease of CpG methylation in *DNMT3A*$^{KO}$ cell lines (Fig. 5E). Consistent with this result, the treatment of 5-AzaC also contributed to a reduction of CpG methylation in *HDAC6* promoter regions (Fig. 5E). Importantly, ChIP results demonstrated that knockout of *DNMT3A* could result in an enrichment of RUNX1 on the promoter region of *HDAC6* in both NCI-H460 and NCI-H1299 cell lines (Fig. 5G). Consistent with the above data, the GEPIA database analyzed results demonstrated that the expression of *RUNX1* was positively related to the *HDAC6* level, which indicated that RUNX1 might be a transcription activator of *HDAC6* (Fig. 5H). Next, we performed immunohistochemistry to assess the relationship between DNMT3A and HDAC6 in NSCLC patients' tumor tissue. Pearson correlation analysis showed a negative correlation between DNMT3A and HDAC6 in the studied 80 tumor tissues (Fig. 5I), which was consistent with *in vitro* results. Taken together, our results elucidate that inhibition of DNMT3A would induce upregulation of *HDAC6* through reducing promoter DNA methylation status.

### 3.7. *DNMT3A deficiency results in HDAC6−VHL−HIF-1 axis activation*

To identify HDAC6 targets in *DNMT3A*-deficient NSCLC cells, we performed RNA sequencing analysis in H460 parental cells, H460-*DNMT3A*$^{KO}$ cells, and WT-161 treated *DNMT3A*$^{KO}$ cells. Since DNMT3A is a DNA methyltransferase and possible gene silencing function[36], we first focused our analysis on the upregulated genes in *DNMT3A*-deficient cells. Our results showed that there were 1165 upregulated genes in H460-*DNMT3A*$^{KO}$ cells relative to parental cells. Next, in view of the selectivity anti-growth action of HDAC6 inhibition, we analyzed the down-regulated genes in HDAC6 inhibitor WT-161 treated *DNMT3A*$^{KO}$ cells as compared with vehicle control. There were 1966 down-regulated genes in WT-161 treated cells. Notably, there were 465 converged genes in both groups, suggesting their crucial role in this synthetic lethal interaction (Fig. 6A). Integrated KEGG pathway and Gene set enrichment analysis (GSEA) revealed that the converged genes were significantly enriched in pathways related to HIF-1, a well-known oncogenic pathway (Fig. 6B). To further explore the relationship between HDAC6 inhibition and the HIF-1 pathway, we next detected the expression levels of some HIF-1 target genes, in the WT-161 treated *DNMT3A*$^{KO}$ cell lines (Supporting Information Fig. S7A and S7B). Besides, we also detected the expression of HIF-1$\alpha$ and VHL in cells under normoxia or hypoxia and analyzed the expression of *HIF-1α* and *VHL* in patients through the cBioPortal database. The results showed that *DNMT3A* deletion or loss of function resulted in high expression of *HIF-1α* and low expression of *VHL* (Fig. S7C−S7E). The role of HIF-1 in *DNMT3A*/*HDAC6* synthetic lethal was confirmed by cell viability assay. Our results indicated that knockdown of *DNMT3A* by specific siRNA could enhance the inhibitory action of WT-161 in H460 cell lines, which was consistent with our previous results. In contrast to H460 parental cells, the enhanced inhibitory action between WT-161 and *DNMT3A* siRNA disappeared in *HIF-1α* knockout H460 cell lines (Fig. 6C). Similar results were obtained in colony formation assays (Fig. 6D). The above results suggest that the synthetic lethal action of *DNMT3A*/*HDAC6* is dependent on the HIF-1 pathway. According to GSEA data, the HIF-1 pathway was inhibited by WT-161 treatment, thus we next investigated whether

*DNMT3A*$^{KO}$ cells after treatment with PX-478 (25 μmol/L for H460, 6 μmol/L for H1299) or LW6 (15 μmol/L for H460 and H1299). (G) A mouse xenograft model was established using NCI-H460 parental and *DNMT3A*$^{KO}$ cells ($n = 5$). The column chart showed the relative growth inhibition after treatment with PX-478 (15 mg/kg, five times per week). The expression of DNMT3A and cleaved PARP in xenografts was analyzed by Western blot. Data are presented as means ± SEM ($n = 3-5$). $^{*}P < 0.05$, $^{**}P < 0.01$, $^{***}P < 0.001$, compared with control group. $^{\#}P < 0.05$, $^{\#\#\#}P < 0.001$, compared with the indicated group. *P* values were determined using Student's *t*-test (independent samples *t*-test).

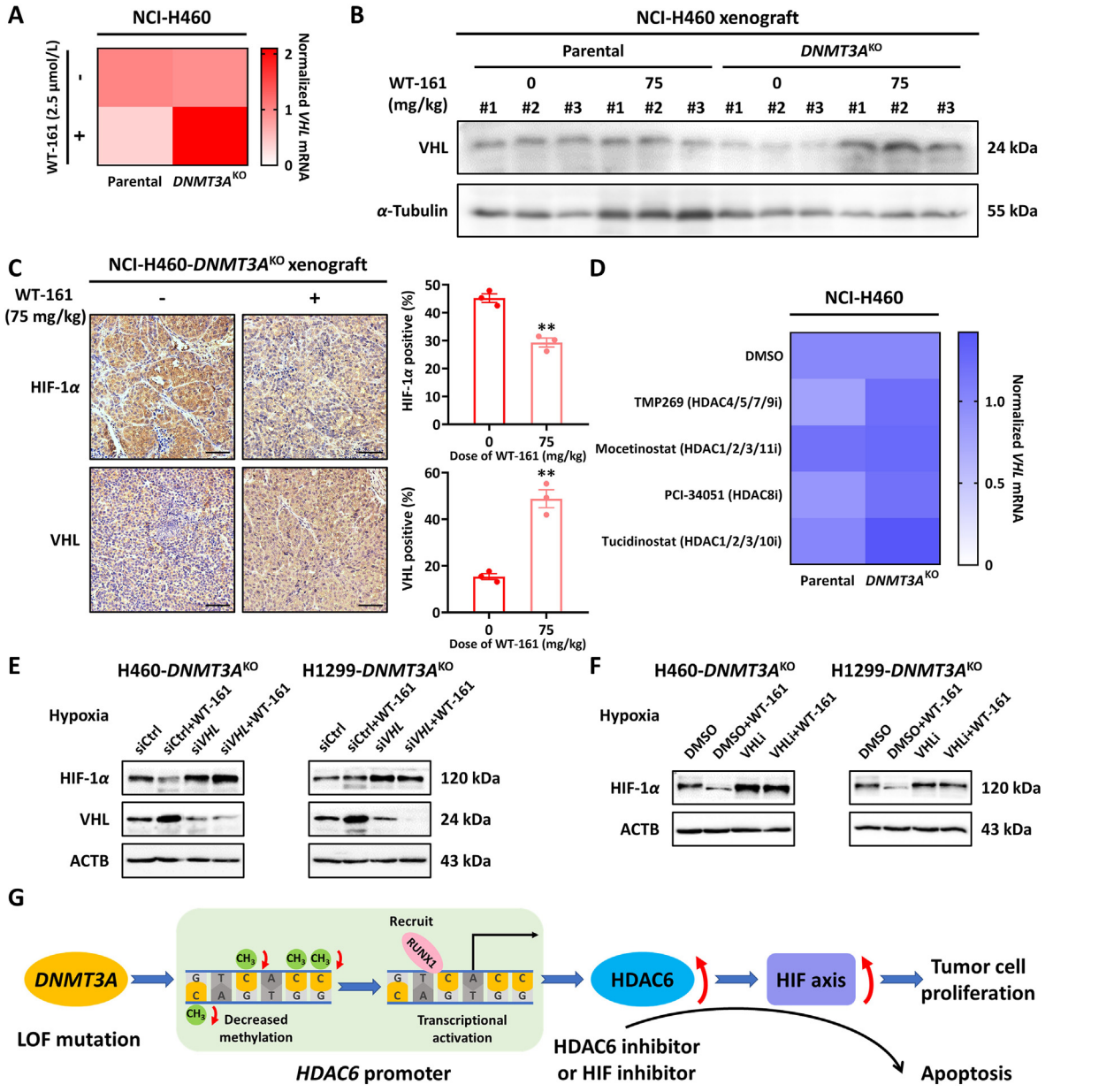


**Figure 7** Increased expression level of VHL after treatment with WT-161. (A) Changes of *VHL* mRNA expression in NCI-H460 parental and *DNMT3A*$^{KO}$ cells after WT-161 treatment (2.5 μmol/L, 48 h). (B) Detection of VHL protein expression in parental and *DNMT3A*$^{KO}$ tumor tissues treated by WT-161 (75 mg/kg, 21 days) by Western blot. (C) Expression of HIF-1α and VHL in tumor tissue of xenograft mice by IHC assay. Scale bars, 50 μm. (D) Effects of inhibitors of other HDAC subtypes (HDAC 4/5/7/9 inhibitor: TMP269, HDAC 1/2/3/11 inhibitor: Mocetinostat, HDAC 8 inhibitor: PCI-34051, HDAC 1/2/3/10 inhibitor: Tucidinostat, 2.5 μmol/L, 48 h) on *VHL* mRNA expression levels. (E, F) The effect of HDAC6 inhibitor WT-161 (2.5 μmol/L, 48 h) on HIF-1α expression after *VHL* siRNA (100 nmol/L, 48 h) or VHL inhibitor VH-298 (40 μmol/L, 48 h) treatment under hypoxia. (G) Schematic diagram showing the increase of HDAC6 induced by *DNMT3A* loss, which leads to HIF axis activation. Data are presented as means ± SEM ($n = 3$). $^{**}P < 0.01$. *P* values were determined using Student's *t*-test (independent samples *t*-test).

inhibition of the HIF-1 pathway could mimic the WT-161 function. The results revealed that treatment with various HIF-1 inhibitors, including PX-478 and LW6, could obviously reduce colony formation in *DNMT3A*$^{KO}$ NSCLC cell lines as compared with those in parental NSCLC cell lines (Fig. 6E). Additionally, FACS analysis also demonstrated that HIF-1 inhibitors could selectively induce cell apoptosis in *DNMT3A*$^{KO}$ NSCLC cells (Fig. 6F). HIF-1 pathway exhibits its function through regulating the tumor microenvironment, therefore we next investigated the role of the HIF-1 pathway in *DNMT3A*/*HDAC6* synthetic lethal

interaction using a xenograft mouse model. Consistent with our previous results, HIF-1 inhibitor PX-478 treatment would result in an obvious reduction of tumor growth in the *DNMT3A*$^{KO}$ xenograft model, with an inhibition rate of 86.35% and no gross toxicity (Supporting Information Fig. S8). However, the antitumor efficacy of PX-478 was significantly attenuated, with an inhibition rate of 29.74%, in the DNMT3A parental xenograft model (Fig. 6G). Consistent with tumor inhibitory efficacy, treatment with PX-478 also significantly induces cleavage of PARP, an apoptosis biomarker of tumor tissues in the *DNMT3A*$^{KO}$ xenograft model (Fig. 6G). These data clarified that the block of the HIF-1 pathway owned a similar biology function with HDAC6 inhibition in *DNMT3A*-deficient cells.

Von Hippel-Lindau (*VHL*) is a tumor suppressor gene, that is highly expressed in normal tissues and benign tumors but decreased in a variety of malignant tumors[37]. Lots of studies have shown that the deficiency of *VHL* tumor suppressor gene can inhibit the degradation of HIF-1$\alpha$, thereby increasing the expression of HIF-1$\alpha$ and causing a series of changes in cells[38]. Based on this, we wondered whether the down-regulation of HIF-1 expression caused by HDAC6 inhibitor in *DNMT3A*$^{KO}$ cells was related to the change of VHL expression. We detected the mRNA and protein expression of *VHL* in H460/H1299 cells and H460 tumor tissues after WT-161 treatments, and the results showed that the mRNA level of *VHL* increased after WT-161 treated *DNMT3A*$^{KO}$ cells (Fig. 7A). In addition, we detected the expression of HIF-1$\alpha$ and HIF-1$\beta$ in cells under hypoxia. The results showed that the expression of HIF-1$\alpha$ in *DNMT3A* knockout cells increased, while the expression of HIF-1$\alpha$ decreased with the addition of WT-161, and the expression of HIF-1$\beta$ did not change significantly (Supporting Information Fig. S9). Similarly, the level of VHL protein in *DNMT3A*$^{KO}$ tumor tissues after WT-161 treatment also increased, and HIF-1$\alpha$ expression was down-regulated (Fig. 7B and C). In addition, we also found that inhibitors of other subtypes of HDAC had no significant effect on the mRNA expression level of *VHL* in *DNMT3A*$^{KO}$ cells (Fig. 7D). These results indicated that HDAC6 inhibitor WT-161 induced the down-regulation of HIF-1 by upregulating the expression of VHL in *DNMT3A*$^{KO}$ cells. In order to explore whether the HIF-1$\alpha$ regulation by HDAC6 inhibition is dependent on VHL. We treated the cells with *VHL* siRNA to investigate whether HDAC6 inhibitors can still affect the expression of HIF-1$\alpha$ under the condition of silencing *VHL*. The results showed that the expression of HIF-1$\alpha$ was not affected by the addition of WT-161 after transient silence of *VHL* under hypoxia (Fig. 7E). We also used a VHL inhibitor and observed the same phenomenon (Fig. 7F). Together, the above results demonstrate that the synthetic lethal action of *DNMT3A*/*HDAC6* is mediated by the VHL−HIF-1 pathway.

## 4. Discussion

There has been a growing interest in using synthetic lethality to identify personalized treatment strategies for cancers with specific genetic defects[39,40]. DNMT3A, a DNA methyltransferase enzyme, was reported to own a relatively high mutation rate in various malignant tumors[20]. Patients with *DNMT3A* mutations, mostly loss-of-function mutation, usually predict a bad prognosis[41]. However, the role and therapeutic value of *DNMT3A* mutation were still not well known. Here, we demonstrated that *DNMT3A* owned a tumor suppressor function in lung cancer. Using the epigenetic inhibitors library, a synthetic lethality interaction between *DNMT3A* and *HDAC6* in lung cancer was identified. Mechanistically, *DNMT3A* loss results in the upregulation of *HDAC6* by decreasing its promoter methylation level and enhancing its transcription activation. As a result, the oncogenic HIF-1 pathway is activated in *DNMT3A*-deficient cell lines. Treatment with HDAC6 inhibitor could retard tumor growth *in vitro* and *in vivo* in *DNMT3A*-deficient NSCLCs via blocking HIF-1 activation (Fig. 7G).

DNMT3A is originally recognized as a pro-oncogenic enzyme, whose overexpression or activation would result in the loss of tumor suppressor genes, such as *p16*[42-44], *CDH1*, and *RASSF1A*[45], through enhancing their promoter CpG methylation. Deng et al.[46] found that silencing of *DNMT3A* with RNA interference inhibited melanoma growth and metastasis. In addition, several reports revealed that overexpression of *DNMT3A* might be associated with malignant characteristics such as high invasiveness and recurrence in melanoma, vulvar squamous cell carcinomas[47], and pituitary adenomas[45]. Paradoxically, several studies have shown that deletion of *DNMT3A* will contribute to tumor progression in various tumors[21]. Here, we verified that knockout of *DNMT3A* in NSCLC cell lines led to malignant phenotypes, including proliferation, self-renewal, and multiple drug resistance. Furthermore, clinical study data showed that NSCLC patients with loss of *DNMT3A* might have a bad prognosis. Taken together, our results demonstrate that *DNMT3A* displays a tumor suppressor role in NSCLC, which suggests the function of *DNMT3A* is highly specific, depending on the tissue and cell type.

Tumor suppressor genes are usually considered undruggable. Recently, the success of synthetic lethality provides a promising approach to target tumor suppressor genes. It is reported that DNMT3A executes its function dependent on interaction and regulation by the other epigenetic enzymes, such as EZH2[48] and DNMT1[11]. Therefore, we identified a synthetic lethal interaction partner of *DNMT3A* with a chemical epigenetic inhibitors screen. Our finding disclosed that pharmacology inhibition of HDAC6 selectively reduced the growth and survival of *DNMT3A*-deficient NSCLC cells and mouse models. Although we found that multiple HDAC6 inhibitors (WT-161, SW-100, CAY10603) differed in the strength of their effects on DNMT3A (Fig. 3B), all three inhibitors specifically target HDAC6, so differential effects due to target inconsistency are essentially ruled out. We speculate that the reason for the difference in the effects of HDAC6-specific inhibitors may be related to the potency, efficacy, and distribution of the drugs *in vivo*. Some researchers have demonstrated the anticancer activity of WT-161 in human multiple myeloma cell xenograft mouse model[49]. It has also been reported that WT-161 and the BET inhibitor have synergistic anti-tumor efficacy against osteosarcoma xenografts, and their combined therapy may be a potential therapeutic strategy[50]. It shows that WT-161 has the strongest effect *in vivo*, which suggests that WT-161 has a better druggability.

Integrated analysis of transcription, protein interaction, and bisulfite sequencing revealed that *DNMT3A* knockout decreased promoter methylation of *HDAC6* and increased its transcription activation of RUNX1. As a result, the upregulation of HDAC6 induced the malignant phenotype of NSCLCs. Thus, inhibition of HDAC6 would lead to selective death in *DNMT3A*-deficient cells. In fact, the epigenetic-based synthetic lethality of *DNMT3A*/*HDAC6* can be extended to other epigenetic pairs[31], such as *EZH2*/*ARIDA*[30], *SMARCB*/*HDAC*[51], CREBBP/p300[52], and H3K27me/IDH[53]. Our results elucidate that the synthetic lethal-based DNA methylation and histone acetylation regulation might be a novel potential strategy. Therefore, deeply digging into the epigenetic synthetic lethality interaction would pave a new pathway for the precision treatment of cancer.

We disclose a mechanism by which HDAC6 inhibition reduces *DNMT3A*-deficient NSCLC growth and survival in a HIF-1-dependent manner. It is well known that the HIF-1 signaling pathway plays a crucial role in the development and progression of cancer by regulating its target genes, including angiogenesis-related genes, proliferation-related genes, and apoptosis-related genes[54-56]. In the present study, our finding indicates that the deletion of *DNMT3A* as a priming factor causes activation of the HIF-1 pathway in cells, but it is inhibited after treatment with HDAC6 inhibitor. The epigenetic regulation of HIF-1 has been reported by several groups. Wang et al.[57] revealed that EZH2 could reduce transcription of *HIF-1* and suppress cancer cell adaption to hypoxia. Chen et al.[58] disclosed that epigenetic reader ZMYND8 interacted with HIF-1 and enhanced elongation of the global HIF-induced oncogenic genes. Recently, a study demonstrated that HDAC6 inhibitor Tubastatin A suppressed Th17 cell function via downregulating HIF-1$\alpha$ pathway[59], which was consistent with our finding. Moreover, we found that HIF-1 is regulated by HDAC6, which may be caused by the down-regulation of VHL[60]. It is reported that the decrease of VHL expression or the loss of its function leads to the activation of HIF-1$\alpha$[6], and HDAC6, a subtype of HDAC II, is known to alter protein function by affecting the level of acetylation of histone or non-histone (the primary mode) substrates, may also be negatively correlated with VHL regulation. However, some researchers pointed out that HDAC6 directly acetylated HIF-1$\alpha$ to affect the protein expression[61], and there is also evidence that HDAC6 affects the stability of HIF-1$\alpha$ protein by acetylating HSP90[62]. It suggests that the regulatory function and state of acetylation modification may be different in diverse cellular environments, which further illustrates the complexity of epigenetic regulation[63,64]. The regulation of HIF-1$\alpha$ by HDAC6 is mainly accomplished through the classical VHL under our research conditions, which complements another regulation mode between HDAC6 and HIF-1$\alpha$. The specific in-depth mechanism of HDAC6 regulating VHL has to be investigated subsequently. Notably, our results indicate whether HDAC6 inhibitor or HIF-1 inhibitor could selectively retard the tumor growth in *DNMT3A*-deficient NSCLC *in vitro* and *in vivo*. Considering that several HDAC6/HIF-1 inhibitors are currently in clinical trials, our results provide a rationale for their application in *DNMT3A*-deficient tumors.

## 5. Conclusions

We have identified HDAC6 as a crucial factor in maintaining the growth of *DNMT3A*-deficient NSCLCs in a HIF-1-dependent manner, which offers opportunities to gain new insights on the molecular cross-talks among epigenetic regulation enzymes. Our findings introduce a potential therapy paradigm for treating *DNMT3A*-deficient cancers like NSCLC.

## Acknowledgments

This work was supported by grants from the National Natural Science Foundation of China (82272725 to Chunfu Wu, 82073320 to Lihui Wang), "Xingliao Talents" Program of Liaoning Province (No. XLYC1902008 to Lihui Wang, China) and Natural Science Foundation of Shenyang (22-315-6-11 to Lihui Wang, China).

## Author contributions

Jiayu Zhang: Writing − original draft, Visualization, Supervision, Methodology, Investigation, Data curation. Yingxi Zhao: Validation, Data curation. Ruijuan Liang: Visualization, Validation, Methodology, Investigation, Data curation. Xue Zhou: Writing − original draft, Visualization, Validation, Methodology, Investigation, Data curation. Zhonghua Wang: Validation, Investigation. Cheng Yang: Validation, Methodology, Investigation. Lingyue Gao: Visualization. Yonghao Zheng: Validation, Data curation. Hui Shao: Validation, Data curation. Yang Su: Supervision, Investigation. Wei Cui: Supervision, Investigation. Lina Jia: Supervision, Investigation. Jingyu Yang: Supervision. Chunfu Wu: Supervision, Funding acquisition. Lihui Wang: Writing − review & editing, Writing − original draft, Supervision, Project administration, Funding acquisition, Conceptualization.

## Conflicts of interest

The authors declare no conflicts of interest.

## Appendix A. Supporting information

Supporting information to this article can be found online at https://doi.org/10.1016/j.apsb.2024.08.025.

## References

1. Siegel RL, Miller KD, Fuchs HE, Jemal A. Cancer statistics, 2022. *CA Cancer J Clin* 2022;**72**:7−33.
2. Alexandrov LB, Kim J, Haradhvala NJ, Huang MN, Tian Ng AW, Wu Y, et al. The repertoire of mutational signatures in human cancer. *Nature* 2020;**578**:94−101.
3. Martinez-Jimenez F, Muinos F, Sentis I, Deu-Pons J, Reyes-Salazar I, Arnedo-Pac C, et al. A compendium of mutational cancer driver genes. *Nat Rev Cancer* 2020;**20**:555−72.
4. Harrison PT, Vyse S, Huang PH. Rare epidermal growth factor receptor (EGFR) mutations in non-small cell lung cancer. *Semin Cancer Biol* 2020;**61**:167−79.
5. Hu J, Cao J, Topatana W, Juengpanich S, Li S, Zhang B, et al. Targeting mutant p53 for cancer therapy: direct and indirect strategies. *J Hematol Oncol* 2021;**14**:157.
6. Chakraborty AA, Nakamura E, Qi J, Creech A, Jaffe JD, Paulk J, et al. HIF activation causes synthetic lethality between the VHL tumor suppressor and the EZH1 histone methyltransferase. *Sci Transl Med* 2017;**9**:eaal5272.
7. Kouzarides T. Chromatin modifications and their function. *Cell* 2007;**128**:693−705.
8. Bates SE. Epigenetic therapies for cancer. *N Engl J Med* 2020;**383**:650−63.
9. Chen S, Zhao Y, Liu S, Zhang J, Assaraf YG, Cui W, et al. Epigenetic enzyme mutations as mediators of anti-cancer drug resistance. *Drug Resist Updat* 2022;**61**:100821.
10. Han M, Jia L, Lv W, Wang L, Cui W. Epigenetic enzyme mutations: role in tumorigenesis and molecular inhibitors. *Front Oncol* 2019;**9**:194.
11. Lyko F. The DNA methyltransferase family: a versatile toolkit for epigenetic regulation. *Nat Rev Genet* 2018;**19**:81−92.
12. Chen Z, Zhang Y. Role of mammalian DNA methyltransferases in development. *Annu Rev Biochem* 2019;**89**:135−58.
13. Yu J, Qin B, Moyer AM, Nowsheen S, Liu T, Qin S, et al. DNA methyltransferase expression in triple-negative breast cancer predicts sensitivity to decitabine. *J Clin Invest* 2018;**128**:2376−88.
14. Mattei AL, Bailly N, Meissner A. DNA methylation: a historical perspective. *Trends Genet* 2022;**38**:676−707.
15. Gravina GL, Festuccia C, Marampon F, Popov VM, Pestell RG, Zani BM, et al. Biological rationale for the use of DNA methyltransferase inhibitors as new strategy for modulation of tumor response to chemotherapy and radiation. *Mol Cancer* 2010;**9**:305.

16. Singh M, Kumar V, Sehrawat N, Yadav M, Chaudhary M, Upadhyay SK, et al. Current paradigms in epigenetic anticancer therapeutics and future challenges. *Semin Cancer Biol* 2022;**83**:422−40.
17. Senapati J, Shoukier M, Garcia-Manero G, Wang X, Patel K, Kadia T, et al. Activity of decitabine as maintenance therapy in core binding factor acute myeloid leukemia. *Am J Hematol* 2022;**97**:574−82.
18. Yan P, Frankhouser D, Murphy M, Tam HH, Rodriguez B, Curfman J, et al. Genome-wide methylation profiling in decitabine-treated patients with acute myeloid leukemia. *Blood* 2012;**120**:2466−74.
19. Yan XJ, Xu J, Gu ZH, Pan CM, Lu G, Shen Y, et al. Exome sequencing identifies somatic mutations of DNA methyltransferase gene DNMT3A in acute monocytic leukemia. *Nat Genet* 2011;**43**:309−15.
20. Ley TJ, Ding L, Walter MJ, McLellan MD, Lamprecht T, Larson DE, et al. DNMT3A mutations in acute myeloid leukemia. *N Engl J Med* 2010;**363**:2424−33.
21. Zhang J, Yang C, Wu C, Cui W, Wang L. DNA Methyltransferases in cancer: biology, paradox, aberrations, and targeted therapy. *Cancers (Basel)* 2020;**12**:2123.
22. Setton J, Zinda M, Riaz N, Durocher D, Zimmermann M, Koehler M, et al. Synthetic lethality in cancer therapeutics: the next generation. *Cancer Discov* 2021;**11**:1626−35.
23. Lord CJ, Ashworth A. PARP inhibitors: synthetic lethality in the clinic. *Science* 2017;**355**:1152−8.
24. Kalev P, Hyer ML, Gross S, Konteatis Z, Chen CC, Fletcher M, et al. MAT2A inhibition blocks the growth of MTAP-deleted cancer cells by reducing PRMT5-dependent mRNA splicing and inducing DNA damage. *Cancer Cell* 2021;**39**:209−24.e11.
25. Zhao D, Lu X, Wang G, Lan Z, Liao W, Li J, et al. Synthetic essentiality of chromatin remodelling factor CHD1 in PTEN-deficient cancer. *Nature* 2017;**542**:484−8.
26. Doffo J, Bamopoulos SA, Kose H, Orben F, Zang C, Pons M, et al. NOXA expression drives synthetic lethality to RUNX1 inhibition in pancreatic cancer. *Proc Natl Acad Sci U S A* 2022;**119**:e2105691119.
27. Jo U, Murai Y, Chakka S, Chen L, Cheng K, Murai J, et al. SLFN11 promotes CDT1 degradation by CUL4 in response to replicative DNA damage, while its absence leads to synthetic lethality with ATR/CHK1 inhibitors. *Proc Natl Acad Sci U S A* 2021;**118**:e2015654118.
28. Flemming A. Cancer: an epigenetic target for synthetic lethality. *Nat Rev Drug Discov* 2015;**14**:236.
29. Wang Z, Chen K, Jia Y, Chuang JC, Sun X, Lin YH, et al. Dual ARID1A/ARID1B loss leads to rapid carcinogenesis and disruptive redistribution of BAF complexes. *Nat Cancer* 2020;**1**:909−22.
30. Bitler BG, Aird KM, Garipov A, Li H, Amatangelo M, Kossenkov AV, et al. Synthetic lethality by targeting EZH2 methyltransferase activity in ARID1A-mutated cancers. *Nat Med* 2015;**21**:231−8.
31. Yang H, Cui W, Wang L. Epigenetic synthetic lethality approaches in cancer therapy. *Clin Epigenetics* 2019;**11**:136.
32. Li J, Hlavka-Zhang J, Shrimp JH, Piper C, Dupere-Richer D, Roth JS, et al. PRC2 inhibitors overcome glucocorticoid resistance driven by NSD2 mutation in pediatric acute lymphoblastic leukemia. *Cancer Discov* 2022;**12**:186−203.
33. Albrengues J, Bertero T, Grasset E, Bonan S, Maiel M, Bourget I, et al. Epigenetic switch drives the conversion of fibroblasts into proinvasive cancer-associated fibroblasts. *Nat Commun* 2015;**6**:10204.
34. Russler-Germain DA, Spencer DH, Young MA, Lamprecht TL, Miller CA, Fulton R, et al. The R882H DNMT3A mutation associated with AML dominantly inhibits wild-type DNMT3A by blocking its ability to form active tetramers. *Cancer Cell* 2014;**25**:442−54.
35. Yin Y, Morgunova E, Jolma A, Kaasinen E, Sahu B, Khund-Sayeed S, et al. Impact of cytosine methylation on DNA binding specificities of human transcription factors. *Science* 2017;**356**:eaaj2239.
36. Yang L, Rau R, Goodell MA. DNMT3A in haematological malignancies. *Nat Rev Cancer* 2015;**15**:152−65.
37. Kaelin WG, Maher ER. The VHL tumour-suppressor gene paradigm. *Trends Genet* 1998;**14**:423−6.
38. Kaelin Jr WG. Von Hippel-Lindau disease: insights into oxygen sensing, protein degradation, and cancer. *J Clin Invest* 2022;**132**:e162480.
39. Zhang B, Lyu J, Yang EJ, Liu Y, Wu C, Pardeshi L, et al. Class I histone deacetylase inhibition is synthetic lethal with BRCA1 deficiency in breast cancer cells. *Acta Pharm Sin B* 2020;**10**:615−27.
40. Li K, You J, Wu Q, Meng W, He Q, Yang B, et al. Cyclin-dependent kinases-based synthetic lethality: evidence, concept, and strategy. *Acta Pharm Sin B* 2021;**11**:2738−48.
41. Patel JP, Gonen M, Figueroa ME, Fernandez H, Sun Z, Racevskis J, et al. Prognostic relevance of integrated genetic profiling in acute myeloid leukemia. *N Engl J Med* 2012;**366**:1079−89.
42. Cui C, Gan Y, Gu L, Wilson J, Liu Z, Zhang B, et al. P16-specific DNA methylation by engineered zinc finger methyltransferase inactivates gene transcription and promotes cancer metastasis. *Genome Biol* 2015;**16**:252.
43. Saito Y, Kanai Y, Sakamoto M, Saito H, Ishii H, Hirohashi S. Expression of mRNA for DNA methyltransferases and methyl-CpG-binding proteins and DNA methylation status on CpG islands and pericentromeric satellite regions during human hepatocarcinogenesis. *Hepatology* 2001;**33**:561−8.
44. Lin RK, Hsu HS, Chang JW, Chen CY, Chen JT, Wang YC. Alteration of DNA methyltransferases contributes to 5′CpG methylation and poor prognosis in lung cancer. *Lung Cancer* 2007;**55**:205−13.
45. Ma HS, Wang EL, Xu WF, Yamada S, Yoshimoto K, Qian ZR, et al. Overexpression of DNA (Cytosine-5)-methyltransferase 1 (DNMT1) and DNA (Cytosine-5)-methyltransferase 3A (DNMT3A) is associated with aggressive behavior and hypermethylation of tumor suppressor genes in human pituitary adenomas. *Med Sci Monit* 2018;**24**:4841−50.
46. Deng T, Kuang Y, Wang L, Li J, Wang Z, Fei J. An essential role for DNA methyltransferase 3a in melanoma tumorigenesis. *Biochem Biophys Res Commun* 2009;**387**:611−6.
47. Leonard S, Pereira M, Fox R, Gordon N, Yap J, Kehoe S, et al. Overexpression of DNMT3A predicts the risk of recurrent vulvar squamous cell carcinomas. *Gynecol Oncol* 2016;**143**:414−20.
48. Vire E, Brenner C, Deplus R, Blanchon L, Fraga M, Didelot C, et al. The polycomb group protein EZH2 directly controls DNA methylation. *Nature* 2006;**439**:871−4.
49. Hideshima T, Qi J, Paranal RM, Tang W, Greenberg E, West N, et al. Discovery of selective small-molecule HDAC6 inhibitor for overcoming proteasome inhibitor resistance in multiple myeloma. *Proc Natl Acad Sci U S A* 2016;**113**:13162−7.
50. Yu B, Liu L, Cai F, Peng Y, Tang X, Zeng D, et al. The synergistic anticancer effect of the bromodomain inhibitor OTX015 and histone deacetylase 6 inhibitor WT-161 in osteosarcoma. *Cancer Cell Int* 2022;**22**:64.
51. Muscat A, Popovski D, Jayasekara WS, Rossello FJ, Ferguson M, Marini KD, et al. Low-dose histone deacetylase inhibitor treatment leads to tumor growth arrest and multi-lineage differentiation of malignant rhabdoid tumors. *Clin Cancer Res* 2016;**22**:3560−70.
52. Ogiwara H, Sasaki M, Mitachi T, Oike T, Higuchi S, Tominaga Y, et al. Targeting p300 addiction in CBP-deficient cancers causes synthetic lethality by apoptotic cell death due to abrogation of MYC expression. *Cancer Discov* 2016;**6**:430−45.
53. Habiba U, Sugino H, Yordanova R, Ise K, Tanei ZI, Ishida Y, et al. Loss of H3K27 trimethylation is frequent in IDH1-R132H but not in non-canonical IDH1/2 mutated and 1p/19q codeleted oligodendroglioma: a Japanese cohort study. *Acta Neuropathol Commun* 2021;**9**:95.
54. Chi JT, Wang Z, Nuyten DS, Rodriguez EH, Schaner ME, Salim A, et al. Gene expression programs in response to hypoxia: cell type specificity and prognostic significance in human cancers. *Plos Med* 2006;**3**:e47.
55. Semenza GL. Hypoxia-inducible factors: mediators of cancer progression and targets for cancer therapy. *Trends Pharmacol Sci* 2012;**33**:207−14.
56. Mole DR, Blancher C, Copley RR, Pollard PJ, Gleadle JM, Ragoussis J, et al. Genome-wide association of hypoxia-inducible factor (HIF)-1$\alpha$ and HIF-2$\alpha$ DNA binding with expression profiling of hypoxia-inducible transcripts. *J Biol Chem* 2009;**284**:16767−75.

57. Wang X, Wang Y, Li L, Xue X, Xie H, Shi H, et al. A lncRNA coordinates with Ezh2 to inhibit HIF-1$\alpha$ transcription and suppress cancer cell adaption to hypoxia. *Oncogene* 2019;**39**:1860−74.
58. Chen Y, Zhang B, Bao L, Jin L, Yang M, Peng Y, et al. ZMYND8 acetylation mediates HIF-dependent breast cancer progression and metastasis. *J Clin Invest* 2018;**128**:1937−55.
59. Zhou W, Yang J, Saren G, Zhao H, Cao K, Fu S, et al. HDAC6-specific inhibitor suppresses Th17 cell function *via* the HIF-1$\alpha$ pathway in acute lung allograft rejection in mice. *Theranostics* 2020;**10**:6790−805.
60. Ellis L, Hammers H, Pili R. Targeting tumor angiogenesis with histone deacetylase inhibitors. *Cancer Lett* 2009;**280**:145−53.
61. Qian DZ, Kachhap SK, Collis SJ, Verheul HM, Carducci MA, Atadja P, et al. Class II histone deacetylases are associated with VHL-independent regulation of hypoxia-inducible factor 1 alpha. *Cancer Res* 2006;**66**:8814−21.
62. Zhang D, Li J, Costa M, Gao J, Huang C. JNK1 mediates degradation HIF-1$\alpha$ by a VHL-independent mechanism that involves the chaperones Hsp90/Hsp70. *Cancer Res* 2010;**70**:813−23.
63. Narita T, Weinert BT, Choudhary C. Functions and mechanisms of non-histone protein acetylation. *Nat Rev Mol Cell Biol* 2019;**20**:156−74.
64. Hsieh WC, Sutter BM, Ruess H, Barnes SD, Malladi VS, Tu BP. Glucose starvation induces a switch in the histone acetylome for activation of gluconeogenic and fat metabolism genes. *Mol Cell* 2022;**82**:60−74.e5.